Defect coarsening in a biological system: The vascular cambium of cottonwood trees

Eric M. Kramer* and Joseph V. Groves
Physics Department, Simon's Rock College, 84 Alford Road, Great Barrington, Massachusetts 01230
(Received 16 August 2002; revised manuscript received 28 January 2003; published 29 April 2003)

We present micrographic evidence for the annihilation of topological defect pairs and defect-mediated coarsening in the vascular cambium of cottonwood trees (*Populus deltoides*). We also show that a recently published mathematical model of cell orientation dynamics in the cambium reproduces many qualitative features of the defect coarsening process.

DOI: 10.1103/PhysRevE.67.041914 PACS number(s): 87.18.Hf, 87.18.La, 64.60.Cn

As the branch of a tree expands radially, new wood is added at the circumference through a gradual process of accretion. The tissue responsible is the vascular cambium, a continuous cylindrical sheath that encases the wood of the branch and is only one cell thick (~ 5 μm) in the radial direction [1]. During the growth of new wood the cambium moves outward through the combined action of cell division and cell expansion. Daughter cells left behind differentiate into the various wood elements (the end products of cellular differentiation are called ''elements'' rather than ''cells'' because many undergo programmed cell death at maturity). The majority of wood elements are elongated and arranged in parallel bundles, resulting in the material anisotropy called wood grain. Wood grain is typically straight and parallel to the axis of the branch, but it may be significantly more complicated. Of interest, here, is ''whirled grain,'' common near wounds, knots, and branch junctions, in which grain lines can form closed loops and other patterns [2].

In Ref. [3], we showed that whirled grain in cottonwood trees (*Populus deltoides*) can be interpreted as a partially ordered system with topological defects (see Fig. 1) [3,4]. Most of the observed defects are point disclinations with winding number $c=+1$ or -1, consistent with a two-dimensional vector order parameter. Disclinations with $c=+1/2$ and $-1/2$ are also observed, but these are invariably connected by a common grain line, presumably a linear discontinuity across which the orientation field rotates by π.

It is important to note that the grain defects are consistent with an order parameter in two dimensions, rather than three. This is because the orientation of wood elements is determined by the orientation of the long axis of cambial cells at the time the wood was formed. Since the long axis of cambial cells is constrained to lie in the plane of the cambium, the order parameter is two dimensional [1]. The cambial cells that play a role in wood grain orientation are called fusiform initials. Initials are elongated, with typical dimensions 15 $\times 300$ μm^2 in the plane of the cambium and 5 μm normal to the cambium [1]. The associated order parameter is the *local orientation field*, which may be estimated at any point in the cambium by averaging over the orientation of initials in a neighborhood of size 500 μm. *Grain lines* are the integral curves of the orientation field.

DEFECTS

In Ref. [3], we presented a circumstantial argument that defect coarsening takes place at some locations in the cambium of a cottonwood tree. Here, we report the results of numerous wood dissections that support this idea. In cottonwoods, whirled grain forms as the cambium grows over the remains of dead branch or abscission zone to form a knot. In all cases examined, we found that the density of topological defects near an encased branch or abscission zone was higher than 1 mm^{-2}. In wood farther from the encased branch (formed at a later time), the defect density decreased to 1 cm^{-2} or less. The grain of a knot eventually returns to a straight, defect-free state. Small knots (<5 mm) take just a few years to eliminate all defects, while some larger knots (3–4 cm) still contain defects after 20 yr of additional radial growth.

Figure 2 shows micrographic evidence for a growing length scale in a healing knot. The horizontal striping is due to differences in grain orientation relative to the plane of the image. Regions with grain oriented parallel to the plane of the image are more reflective and appear brighter than re-

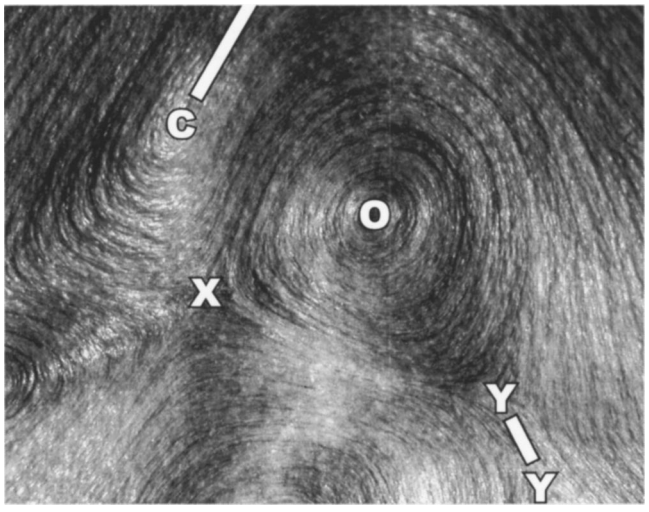

FIG. 1. Whirled wood grain at the surface of a debarked cottonwood log. Point disclinations are marked by an $X(c=-1)$, $O(c=+1)$, $Y(c=-1/2)$, or $C(c=+1/2)$. Linear discontinuities are marked by line segments. Width of figure=11 mm.

*Corresponding author. Email address: ekramer@simons-rock.edu

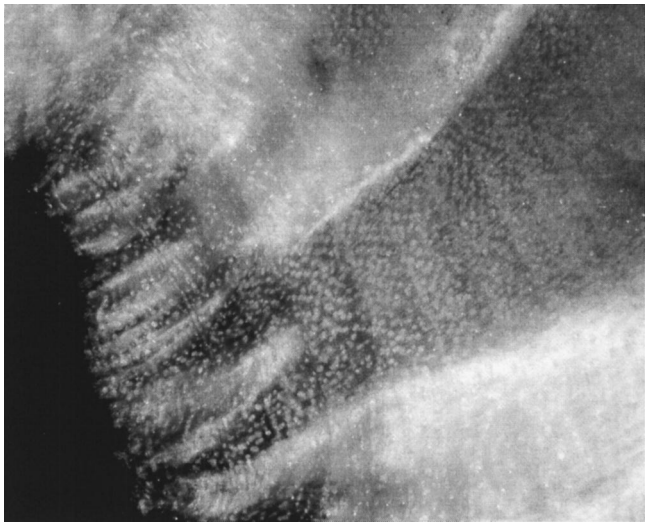

FIG. 2. Cross section through a knot, normal to the axis of the branch. The black region at left is the wood of a dead branch. Low contrast vertical bands are the annual growth rings, with the oldest at left. High contrast striping, running largely left to right, is due to curvature in the grain. Width of figure = 9 mm.

gions with grain normal to the plane. The mean distance between stripes, as measured on a line parallel to the annual growth rings, is thus a measure of the curvature of the grain. In wood near the encased branch the distance between stripes is roughly 0.3 mm. The distance increases as the cambium grows away from the branch, indicating a gradual decrease in grain curvature.

Disclinations can only be eliminated from the cambium through the approach and annihilation of two or more defects whose winding numbers sum to zero [4]. Figure 3 illustrates the annihilation of a typical $+1$ and -1 defect pair. The micrographs depict wood grain on two fracture surfaces, spaced roughly 2 mm apart in the radial direction. As the defect cores approach a separation of 1 mm, the grain lines between them tend to become parallel, giving a ''hairpin'' kink in the grain. At later times the hairpin straightens out. Following an additional 1 mm of radial growth, the grain in this region is straight. This sequence of events is the usual means for elimination of defects from whirled grain and is reproduced in the simulations described below.

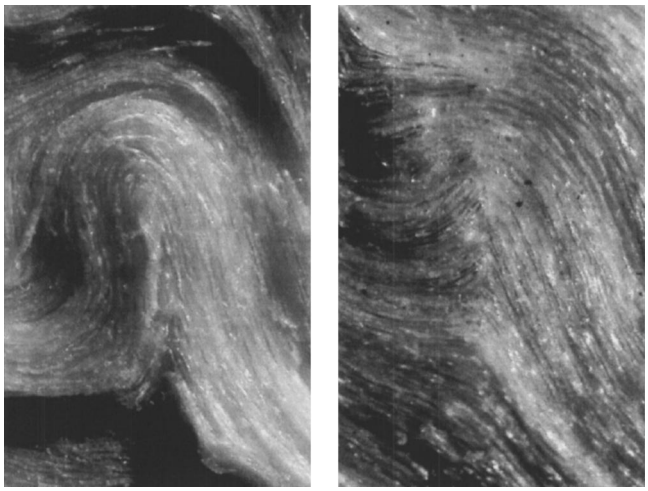

FIG. 3. Micrographs showing two stages in the elimination of a disclination pair. Left: as the $+1$ and -1 pair approach a separation of about 1 mm, the grain lines adopt a ''hairpin'' shape. Shadows are due to an uneven fracture surface. Right: after 2 mm of additional radial growth (2–3 yr), no disclinations are present. Height of figure = 2.6 mm.

THEORY

Before proceeding, we should distinguish the vascular cambium from the *cambial region*. The cambial region is the sheath of tissue (<1 mm thick) that includes both the vascular cambium and adjacent layers of developing cells [1]. The plant hormone indoleacetic acid (IAA), which plays an important role in the orientation of fusiform initials, is distributed throughout the cambial region [5,6]. For technical reasons, the model discussed below uses the concentration of IAA integrated through the thickness of the cambial region as a proxy for the IAA concentration in the vascular cambium. To a first approximation they are proportional [7]. Measured values for IAA concentration in the cambial region of *Populus* fall in the range $m = 10\text{–}40\ \mathrm{ng\,cm^{-2}}$ [6].

A mathematical model that describes the coarse-grained (length scale ~ 0.5 mm) behavior of the orientation field in cottonwood cambium was presented in Ref. [7]. The equation of motion for the local angle of grain orientation $\phi(x,y,t)$ is

$$\frac{\partial \phi}{\partial t} = K\nabla^2 \phi - \mu \nabla_\perp m, \tag{1}$$

where $m(x,y,t)$ is the concentration of IAA in the cambial region, $\nabla_\perp m$ is the component of the gradient perpendicular to the local grain orientation, and K and μ are phenomenological constants. It is helpful to define the unit vector fields $\hat{\mathbf{u}} = \mathbf{x}\cos\phi + \mathbf{y}\sin\phi$ parallel to the grain and $\hat{\mathbf{w}} = -\mathbf{x}\sin\phi + \mathbf{y}\cos\phi$ perpendicular to the grain. Then, $\nabla_\perp m = \hat{\mathbf{w}}\cdot\nabla m$. The first term in Eq. (1) represents a short-range interaction that aligns adjacent initials. The second term represents a chemotactic effect that rotates the initials until they are parallel to the flux of IAA through the cambium [8]. The values for K and μ are set by the biochemical and genetic response of the cambial cells to gradients in the orientation field and IAA concentration, respectively. We estimate K and μ below by comparing observed wood grain patterns with model simulations.

The model also incorporates the fact that cells of the cambial region actively transport IAA parallel to their long axes. The flux of IAA obeys an advection-diffusion equation

$$\mathbf{j} = (-D_\parallel \nabla_\parallel m + \nu m)\hat{\mathbf{u}} + (-D_\perp \nabla_\perp m)\hat{\mathbf{w}}, \tag{2}$$

where $D_\parallel$ and $D_\perp$ are diffusion coefficients, ν is the transport velocity, and $\nabla_\parallel m = \hat{\mathbf{u}}\cdot\nabla m$ is the component of the gradient parallel to the grain. We take $\nu = 10$ mm/h, $D_\parallel = 5.0\ \mathrm{mm^2/h}$, and $D_\perp = 1.2\ \mathrm{mm^2/h}$ [7].

During transport over intracambial distances that are not much larger than the branch circumference, IAA is approximately conserved [9]. The flux thus satisfies the two-dimensional continuity equation $\partial m/\partial t = -\nabla\cdot\mathbf{j}$.

SIMULATIONS

To avoid difficulties with defect pinning in our simulations, we allow the order parameter to have variable length. Unit magnitude is enforced approximately by a ''Mexican hat'' potential [4]. Because $\mathbf{u}$ has one more degree of freedom than $\hat{\mathbf{u}}$, the choice for a modified equation of motion is not unique. The following functional gives reasonable results and reduces to Eq. (1) when $u=1$.

$$F=\int dA\,\frac{K}{2}\left\{(\partial_\alpha u_\beta)^2+\frac{1}{L^2}V(u)\right\}+\mu(\mathbf{u}\cdot\boldsymbol{\nabla}m)\left(\frac{3-u^2}{2}\right), \tag{3}$$

where $V(u)=(1-u^2)^2$ and $\partial\mathbf{u}/\partial t=-\delta F/\delta\mathbf{u}$. It is useful to transform to the dimensionless variables $\mathbf{r}'=\mathbf{r}\nu/D_\parallel$, $t'=tK(\nu/D_\parallel)^2$, and $m'=m/\langle m\rangle$, where $\langle m\rangle$ is any characteristic value of the IAA concentration (we use the mean). Dropping primes, we have

$$\frac{\partial m}{\partial t}=r_t\boldsymbol{\nabla}\cdot\{(\boldsymbol{\nabla}_\parallel m-m)\hat{\mathbf{u}}+(r_D\boldsymbol{\nabla}_\perp m)\hat{\mathbf{w}}\}, \tag{4}$$

$$\frac{\partial\mathbf{u}}{\partial t}=\nabla^2\mathbf{u}+\frac{2}{(L')^2}\mathbf{u}(1-u^2)+\frac{1}{\lambda'}\left\{-(\boldsymbol{\nabla}m)\left(\frac{3-u^2}{2}\right)+(\mathbf{u}\cdot\boldsymbol{\nabla}m)\mathbf{u}\right\}, \tag{5}$$

where $r_t=D_\parallel/K$, $r_D=D_\perp/D_\parallel$, $L'=L\nu/D_\parallel$, and $\lambda'=K\nu/(\mu D_\parallel\langle m\rangle)$ are the four dimensionless numbers that characterize the solutions [10].

Comments.

(i) The ratio r_t characterizes the difference in time scales between changes in the IAA concentration and the much slower changes in the orientation of cambial cells. Note that the model is well defined in the limit $r_t\to\infty$ [set $\partial m/\partial t=0$ in Eq. (4)]. Below, we estimate r_t in cottonwood trees to be 10^5. Our simulations typically approximate the large r_t limit with $r_t=100$. Increasing to $r_t=1000$ gives a negligible change in the numerical solutions.

(ii) The ratio $r_D=0.23$ here.

(iii) L' is the dimensionless core size for defects. Considering that we are coarse graining over a length scale ~ 0.5 mm, $L=0.25$ mm is a reasonable choice. Thus, $L'=0.5$.

(iv) λ' is a dimensionless length scale. It may be determined from observations of a curl localization phenomena as described below.

Our simulations of Eqs. (4) and (5) used a FTCS (forward time, centered space) algorithm as described in Ref. [11]. The fields $m(x,y,t)$ and $\mathbf{u}(x,y,t)$ were discretized on a square lattice with spacing $\Delta x\leqslant 0.2$ mm. Care was taken to ensure that the algorithm conserved IAA up to the round-off error, and runs were made at smaller Δx to check the validity of results.

CURL LOCALIZATION

A quantitative study of cottonwood grain, made by extracting the orientation field from digital micrographs [12], found a prominent curl localization phenomena. As shown in Fig. 4, the curl tends to be concentrated into linear ''bends'' that extend between defect cores. This is a generic feature of the grain, easily detectable once the defect separation exceeds 3–4 mm. Figure 5 shows the curl and divergence of the grain measured transverse to a bend. The curl is sharply peaked. Although the maximum value of the curl varies from bend to bend, the transverse width (full width at half maximum) of the peak is uniformly about 1.0 mm. The divergence may weakly colocalize with the curl, but uncertainties in our data prevent a stronger conclusion.

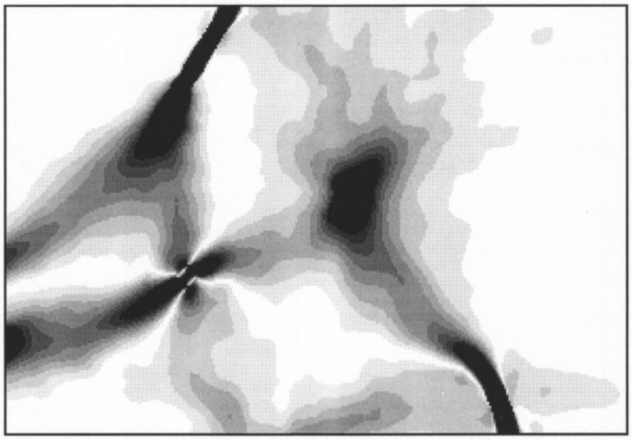

FIG. 4. Magnitude of the curl of the orientation field for the grain shown in Fig. 1. Gray scale increases in steps of 0.25 mm^{-1}. Regions of curl exceeding 1.75 mm^{-1} are black.

These observations are consistent with numerical solutions of the model. We ran a set of simulations on rectangular domains with boundary conditions appropriate to the region between defects and examined the curl and divergence of the steady-state solutions. As shown in Fig. 5, the model shows a qualitatively similar curl localization phenomenon. The divergence (not shown) tends to have a much smaller magnitude except near defect cores.

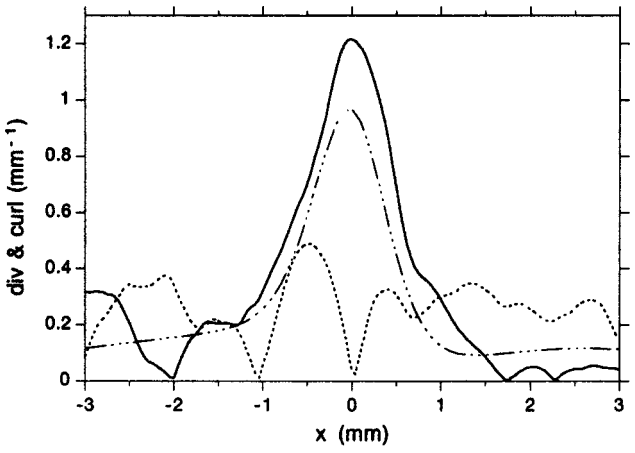

FIG. 5. Magnitude of the curl and divergence transverse to a bend in the grain. Solid line: curl along a line passing through the middle of the linear bend at center right of Fig. 3. Dotted line: divergence along same. Dashed line: steady-state numerical solution to the model showing the same effect. Parameter values: $r_D=0.23$, $L'=0.5$, and $\lambda'=0.1$.

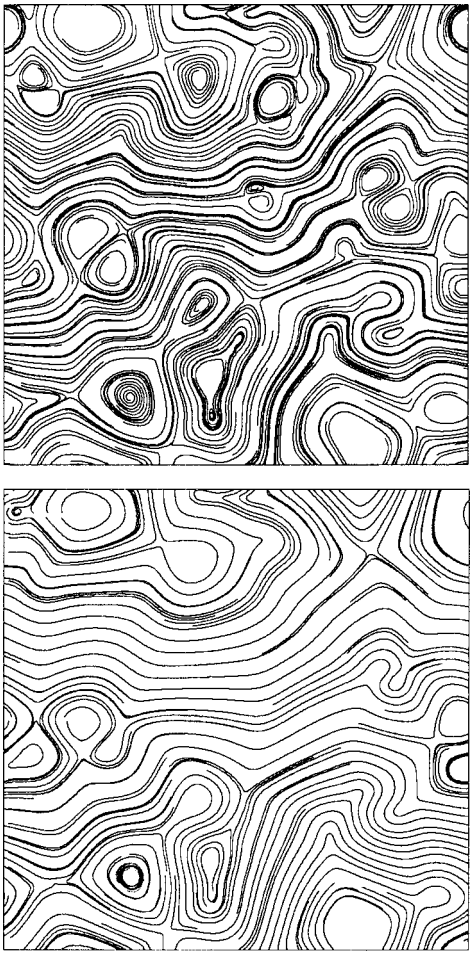

FIG. 6. Grain lines for simulated whirled grain in a square of cambium $24\times24\ \mathrm{mm}^2$ at $t=4$ (top) and 6 (bottom). Parameter values: $r_t=100$, $r_D=0.23$, $L'=0.5$, and $\lambda'=0.1$.

Because curl localization persists far (>2 mm) from defect cores, we expect the properties of bends in the grain to be only weakly dependent on L'. Numerical results confirm this. By contrast, the width of the bend increases approximately linearly with λ'. We find that a value of $\lambda'=0.1$ corresponds to the observed bend width of 1.0 mm.

DEFECT COARSENING

Defect coarsening was simulated on a square domain, typically $24\times24\ \mathrm{mm}^2$, with periodic boundary conditions. The initial conditions were $m=1.0+\alpha$, $\mathbf{u}=(\cos\phi_0,\sin\phi_0)$, where $\alpha(x,y)$ and $\phi_0(x,y)$ were random numbers on the intervals $[-0.1, 0.1]$ and $[-\pi, \pi]$, respectively.

Figure 6 shows two snapshots of a simulated whirled grain pattern as it evolves in time, visualized by drawing sets of grain lines. The patterns show good qualitative resemblance to whirled grain in cottonwoods. Note, in particular, (1) defect pairs typically annihilate through the formation of hairpin kinks in the grain, (2) point disclinations are observed with both integer and 1/2-integer winding number, (3) disclinations with 1/2-integer winding number occur in pairs connected by a grain line that denotes a linear discontinuity in the orientation field, and (4) $+1$ disclinations have grain lines that circle the defect core.

A comparison of our numerical results to observations of defect annihilation in cottonwood permits an estimate of the parameter K. Coarsening simulations show that the elimination of a pair of defects 1 mm apart requires a dimensionless time interval of $\Delta t=1-2$. The same process takes 2–4 yr in cottonwood. Estimating the yearly growing season as 100 days, and recalling the definition of the dimensionless time, we find $K=5\times10^{-5}\ \mathrm{mm}^2/\mathrm{h}=0.5\ \mathrm{mm}^2/\mathrm{yr}$. Substituting into the expressions for r_t and λ', we get $r_t=10^5$ and $\mu=(10^{-3}\ \mathrm{mm/h})/\langle m\rangle$.

It is our hope that future discoveries in the genetics and biochemistry of cambial cells will permit an understanding of the model from first principles. Until then, the model should serve as a guide for a quantitative approach to the dynamics of cambial cell orientation.

ACKNOWLEDGMENTS

We are grateful to Michael Bergman for helpful discussions, and to Simon's Rock College for the support of this research through the provision of a Faculty Development Fund.

[1] P. R. Larson, *The Vascular Cambium* (Springer, New York, 1994); *The Vascular Cambium*, edited by M. Iqbal (Wiley, New York, 1990).
[2] S. Lev-Yadun and R. Aloni, Trees **4**, 49 (1990).
[3] E. M. Kramer, J. Theor. Biol. **200**, 223 (1999).
[4] *Formation and Interaction of Topological Defects*, edited by A.-C. Davis and R. Brandenberger (Plenum Press, New York, 1995).
[5] C. Uggla, E. Mellerowicz, and B. Sundberg, Plant Physiol. **117**, 113 (1998).
[6] H. Tuominen *et al.*, Plant Physiol. **115**, 577 (1997); H. Tuominen *et al.*, *ibid.* **123**, 531 (2000).
[7] E. M. Kramer, J. Theor. Biol. **216**, 147 (2002).
[8] J. M. Harris, *Spiral Grain and Wave Phenomena in Wood Formation* (Springer, New York, 1989); T. Sachs, *Pattern Formation in Plant Tissues* (Cambridge University Press, New York, 1991), and references therein.
[9] E. M. Kramer, J. Theor. Biol. **208**, 387 (2001).
[10] This model is similar to the model of J. Toner and Y. Tu [Phys. Rev. Lett. **23**, 4326 (1995)] for the collective motion of birds. Two notable differences are (i) they do not allow for diffusion of birds within the flock (they take $D_\parallel=D_\perp=0$), and (ii) we do not include an advection term like $(\mathbf{u}\cdot\nabla)\mathbf{u}$ in Eq. (5) since the translational motion of the cambial cells is negligible.
[11] W. Press *et al.*, *Numerical Recipes* (Cambridge University Press, New York, 1989).
[12] Using the program Grain Analysis, to be described separately.